Automated ground-based star-pointing UV–visible spectrometer for stratospheric measurements

Howard K. Roscoe, William H. Taylor, Jon D. Evans, Andy M. Tait, Ray Freshwater, Debbie Fish, E. Kimberly Strong, and Rod L. Jones

A novel automated ground-based star-pointing spectrometer system has been constructed for long-term deployment in Antarctica. Similar to our earlier stellar system, a two-dimensional detector array measures the spectra of the star and the adjacent sky, so that auroral emission from the sky can be subtracted from the stellar signal. Some new features are an altitude–azimuth pointing mirror, so that the spectrometer does not move; slip rings to provide its power thereby avoiding flexing of cables and restriction of all-around viewing; and a glazed enclosure around the mirror to ensure protection from rain and snow, made from flat plates to avoid changing the focal length of the telescope. The optical system can also view sunlight scattered from the zenith sky. The system automatically points and tracks selected stars and switches to other views on command. The system is now installed at Halley in Antarctica, and some preliminary measurements of ozone from Antarctica are shown. © 1997 Optical Society of America

1. Introduction

We have developed a new UV–visible instrument (UVIZ) for measuring atmospheric constituents from spectra of stars at Halley (formerly station Z) in Antarctica. Similar to our earlier instrument,[1] it has the potential of measuring O_3, NO_2, NO_3, and OClO simultaneously. It significantly extends the range of sources and elevation angles at night, providing increased measurement opportunities, because it has sufficient sensitivity to observe stars and planets. This is particularly useful for measurements near the poles in winter when it is dark, when conditions that lead to possible ozone depletion occur. At other seasons it also has potential for measurements of OClO, because OClO amounts increase significantly during the night, and of NO_3, because NO_3 exists only at night.

Similar to our earlier instrument, ozone is measured at visible wavelengths between 450 and 565 nm, where depths of absorption are less than in the UV but signal levels are greater and less light is scattered out of the beam when the star is close to the horizon. This is especially important at Antarctic latitudes, where Sirius, the brightest star in the sky, is too close to the horizon for UV measurements with a good signal-to-noise ratio. Spectra of a star are acquired at low- and high-elevation angles; the ratio of these spectra is independent of absorption in the atmosphere of the star.

Unlike our earlier instrument, the UVIZ can also observe the zenith sky, which allows the full capability of the Systeme Automatique d'Observations Zénithales (SAOZ) spectrometers[2] but with improved signal-to-noise ratio because the detector has less dark current. Because zenith-sky measurements of ozone in the visible can be made at solar zenith angles as large as 91°, these observations can be made for much more of the year in Antarctica than are possible with the Dobson spectrophotometer that observes at UV wavelengths.[3]

Many details of the spectrometer and detector are unchanged (e.g., entrance slit of 2.4 nm FWHM, a 200-grooves/mm grating, 0.55-nm pixel width), but other new features include an adjustable focus, a filter wheel, and a tungsten lamp. The UVIZ is also fully automated and is enclosed in an environmental housing so that it can operate outdoors in extreme conditions. It is now installed at Halley (75.58 °S,

H. K. Roscoe, W. H. Taylor, J. D. Evans, and A. M. Tait are with the British Antarctic Survey, Natural Environment Research Council, Madingley Road, Cambridge CB3 0ET, United Kingdom. R. A. Freshwater, D. J. Fish, E. K. Strong, and R. L. Jones are with the Cambridge Centre for Atmospheric Science, Department of Chemistry, Cambridge University, Lensfield Road, Cambridge CB2 1EW, United Kingdom.

Received 20 March 1996; revised manuscript received 10 October 1996.

0003-6935/97/246069-07$10.00/0

26.77 °W). Here we describe some of these new features and discuss the rationale for their choice. We also show some sample spectra of Sirius and of the zenith sky, together with preliminary amounts of ozone deduced from these spectra.

2. Optics Design

The diameter of the input aperture of the optics is 155 mm, somewhat less than the 300 mm of our earlier instrument. Although this gives smaller signals, this was an important compromise to keep the overall size to reasonable dimensions for an environmentally sealed box and to keep the overall weight below 300 kg so that mounting and installing it were simplified.

The optical design is illustrated in Fig. 1. A novel part of the design is the pointing mirror,[4] that allows the spectrometer to remain stationary while the mirror tracks stars—a spectrometer mounted at the focal plane of an astronomical telescope must swivel with the telescope, which is unreliable for permanent installation. Power for the altitude pointing system and signals from its angle measurement are transferred by way of slip rings, so that again there are no twisting cables and no stops to the all-around view of the mirror. Such a pointing system cannot have a coaligned telescope to sight on the star because the input mirror moves by half of the altitude angle of the input beam. Instead, a beam splitter directs light to a small TV camera designed for astronomical pointing systems (SBIG ST4). The geometry of the pointing mirror means that the horizon rotates as the azimuth changes, so that the error signal from the TV camera must be transformed. This means that the camera's commercial tracking software cannot be used.

Because of probable differential expansion between the glass of the telescope mirrors and the aluminum alloy of their support tube, the relay of the beam from the telescope to the spectrometer is split between two lenses, with approximately parallel light between them; one lens is movable by as much as 15 mm. This compensates for a shift in focus equivalent to a 50 K change in temperature. It also allows us to focus lamps on nearby buildings, as opposed to stars at infinity: such lamps are useful for confirming pointing operation during the permanent daylight of the Antarctic summer.

Similar to our earlier instrument, the UVIZ uses a CCD detector array to measure all the spectrum simultaneously. This prevents scintillation noise and allows measurements to be made when cloud cover varies. Again, the second dimension of the array allows the simultaneous measurement of auroral emission from the sky adjacent to the star, which can then be subtracted from the stellar signal.

Unlike our earlier instrument, a mirror can switch the spectrometer's input beam to different views, bypassing the telescope and pointing mirror. One view, by way of a relay lens and mirror, is through a port on top of the housing that contains a conical Teflon diffuser to observe the UVB intensity from the whole sky with a cosine response. Another view,

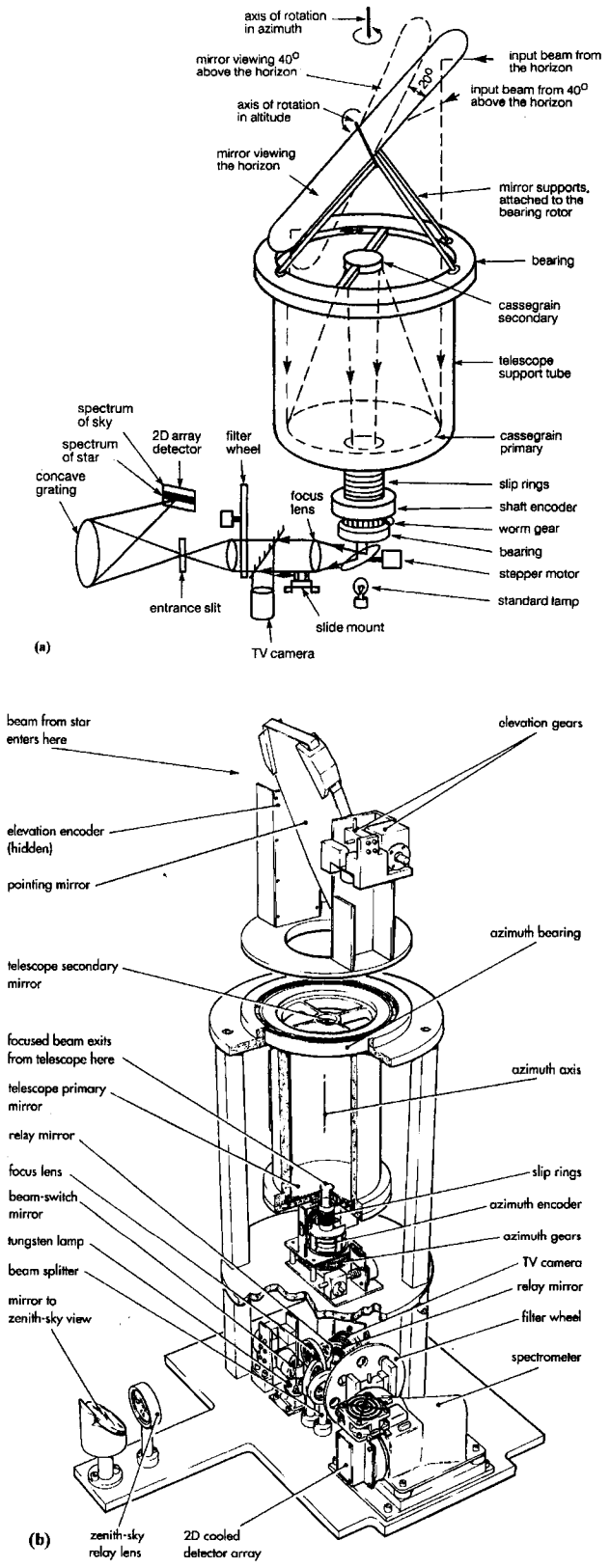

Fig. 1. (a) Schematic and (b) mechanical drawing of the new UV–visible spectrometer for stellar measurements from Halley in Antarctica (UVIZ). This optical scheme allows the spectrometer to be stationary, rather than to swivel with the telescope. The pointing mirror directs light from stars within 40° of the horizon into the telescope, which rotates with the mirror so that slip rings and an azimuth encoder of modest diameter can be used.

also by way of a relay lens and mirror, is through a quartz lens, also on top of the housing; this views sunlight scattered from the zenith sky. The quartz lens degrades slightly the otherwise narrow field of view but is a simple way of ensuring that water from snow melting on the lens would not stay.

The beam-switch mirror can also view a tungsten lamp that acts as a spectrally smooth emitter to correct variations in sensitivity of each pixel relative to its neighbors[1] (known in the astronomy community as flat fielding). This is important as these sensitivity variations add a large and systematic error to each spectrum. Without the tungsten lamp measurements, when dividing by a spectrum at high stellar elevation, these errors can be corrected only if both spectra have identical wavelength calibrations.

When one uses the tungsten lamp, the grating must be uniformly illuminated otherwise the convergence of the signal on the detector will differ from that of stellar and other observations, so that the relative gain of its pixels will differ. Hence a quartz diffuser is mounted on a filter wheel that can be rotated into the beam in front of the spectrometer slit. Other components of the wheel are

(i) a blue filter with diffuser to reduce the intensity of red light from the tungsten lamp, so that useful signals can be obtained simultaneously from 400 to 800 nm;

(ii) a bluer filter to remove stellar light at wavelengths longer than 390 nm to cut down the stray light when one attempts to measure OClO;

(iii) a yet-bluer filter and a diffuser, used when observing the tungsten lamp in this OClO region;

(iv) a violet filter to remove sunlight at wavelengths longer than 350 nm when one observes UVB;

(v) a yellow filter to remove UV light in second order from the NO_3 region near 663 nm, thought to be important for accurate measurements of NO_3.

Each filter is made of colored glass: colored glasses have negligible fine structure in their spectra, so that changes in their spectra with time or temperature would have little effect on the optical depths of atmospheric gases deduced. The well-known dependence of color glass transmission on temperature is not important unless temperatures change significantly during a night, because the ratio of spectra to that of the same source high in the sky is always used for analysis. In any case the color glass transmission does not contain features with fine structure so that features are ignored in the differential analysis scheme described below.

3. Control System

The new system is automated by means of a desktop PC indoors and a PC inside the spectrometer housing that is located outdoors. The outdoor PC is complementary metal-oxide semiconductor that continues to function at temperatures below −20 °C. The computers communicate by way of fiber-optic links (RS232) to reduce the possibility of rf interference from the radar at Halley. The fiber-optic links also reduce problems of static, important at Halley because it is on an ice shelf so that there is no proper ground and because wind-blown snow below −10 °C can create significant static buildup. The detector has its own proprietary control box that uses a programmable-array-logic chip to execute commands and communicate with the indoor computer by way of a bidirectional coaxial link at 10 Mbits/s. The TV camera also has its own proprietary control box that uses an 8051 microcontroller, which had been tested at −20 °C, to communicate by RS232 link with either computer.

The software that operates the system is split between indoor and outdoor computers. An appealing feature of using two similar computers is that modules can be operated from either with little modification necessary in order to exchange their location. The programs are in Microsoft-C 6.00; they operate the mechanisms and control the detector from one suite. The upper part of the screen on the indoor computer displays real-time status of selected instrument functions, and the lower part allows the control and displays the status of either the mechanisms or the detector. These alternatives are possible because only during tracking are mechanisms moved while the detector is being operated. During acquisition of stellar spectra, control of tracking passes to the outdoor computer. With this division of software between the two computers, no multitasking is needed in either.

4. Environmental Housing and Mount

The system is mounted in a box with removable insulated panels, as illustrated in Fig. 2. The panels are sealed against snow by silicon rubber gaskets. Their inner faces are of an aluminum alloy to improve rf screening; their outer faces are white plastic to reflect sunlight. The outer face of the upper panel is clad in a white-painted aluminum alloy of 3-mm thickness, and it contacts an internal channel through which a thermostated fan blows inside air to provide cooling when temperatures inside the box rise above 10 °C. This condition is easily reached at Halley on a sunny day in mid-summer in spite of maximum external temperatures below −2 °C.

Although many components in the system have been tested at −40 °C, we reduced the chance of low-temperature failure by providing some general heating inside the box with a cutoff at ~0 °C. The spectrometer itself is separately thermostated at 25 °C to reduce drifts in wavelength calibration. Figure 3 shows how this temperature control system coped well until external temperatures fell below −40 °C. Because we chose a simple control system for improved reliability, a more powerful spectrometer heater that could cope with lower temperatures would also lead to larger oscillations in temperature at the control point. The computers still communicated when external temperatures were below −50 °C.

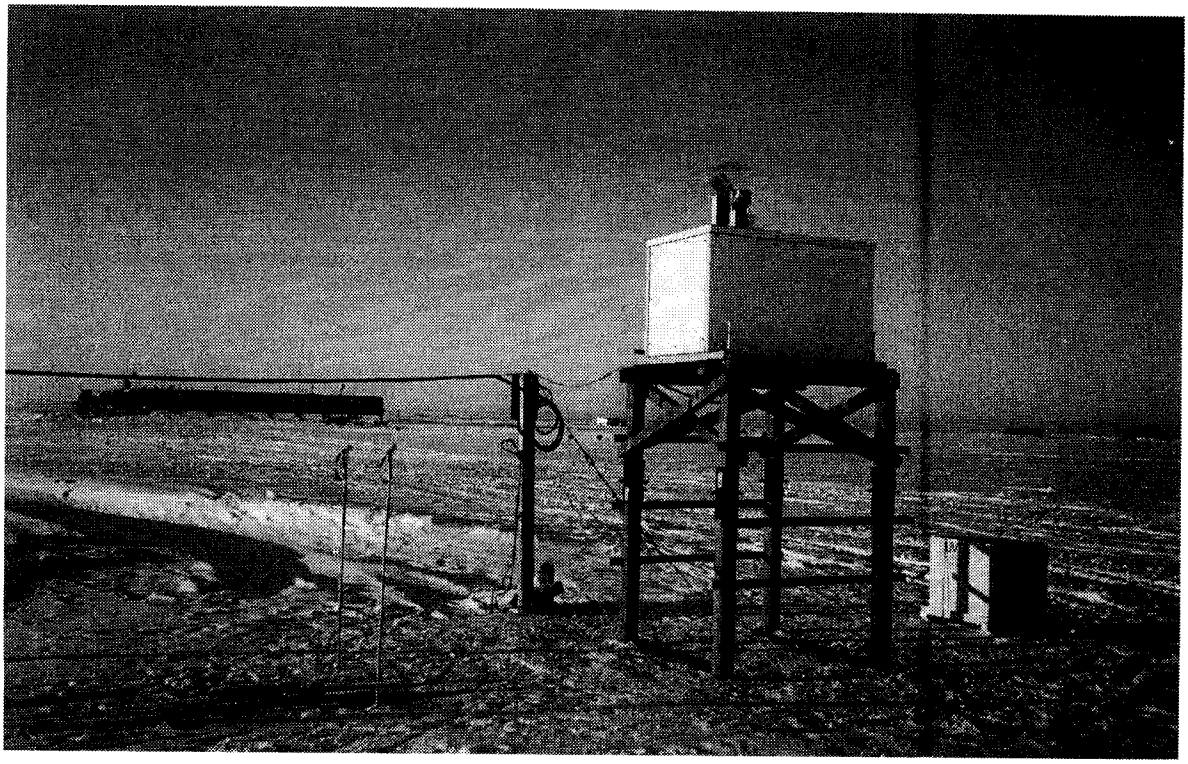

Fig. 2. UVIZ in its environmental housing at Halley. The housing is waterproof and snow proof and contains heating and cooling systems. The top part of the timber frame was triangulated for extra rigidity, and the verticals can be split to insert extra lengths after each year's snow accumulation. A third of the frame is buried to rest on the more stable snow below the surface.

At Halley in Antarctica, there is no rock upon which to mount apparatus, only an ice shelf of ~100-m thickness. The shelf receives an annual snowfall that compacts to ~1.2 m during the course of the year. The surface is not sufficiently rigid for mounting apparatus that must be stable to within a few tenths of a degree. If apparatus is flush with the surface, it creates large drift tails that would probably submerge the apparatus within the year.

Hence we constructed a timber frame that rests on plates buried at a depth of 1.5 m and extended 1.7 m above the surface so that there would still be a gap of at least 0.5 m below the apparatus after 1 year. The frame was triangulated for increased rigidity, both in

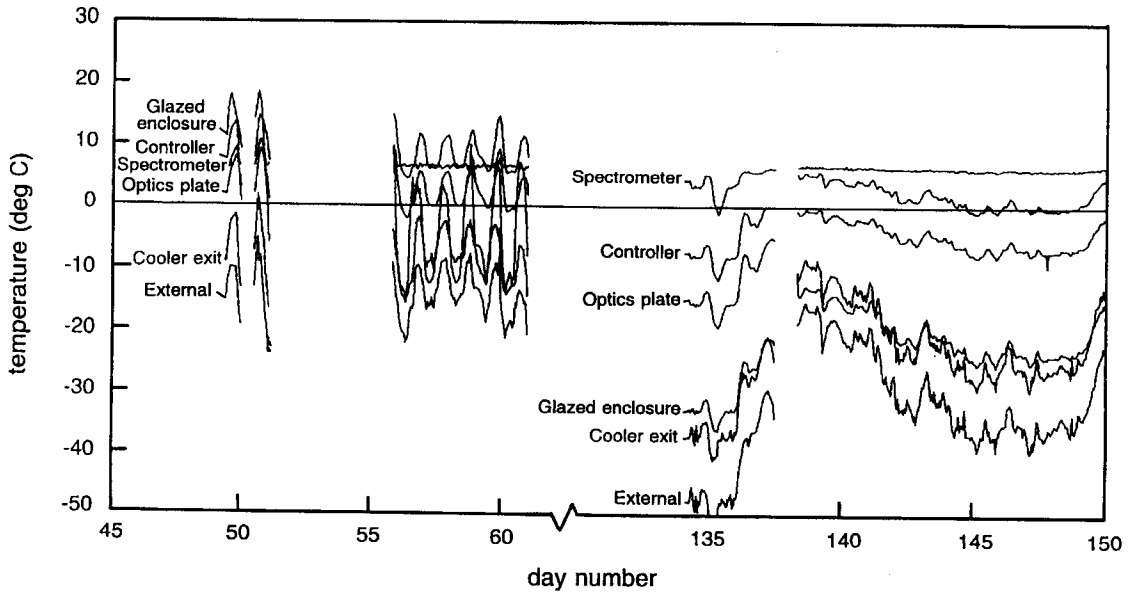

Fig. 3. Temperatures in the UVIZ during its first autumn of operation at Halley. Gaps in data occurred during extended fault-finding operations. The temperature of the spectrometer became uncontrolled at external temperatures below −40 °C, and above −10 °C in strong sunlight in summer, resulting in a larger drift in wavelength calibration. Although wavelengths are determined for each spectrum, errors in wavelength are larger when drift is larger.

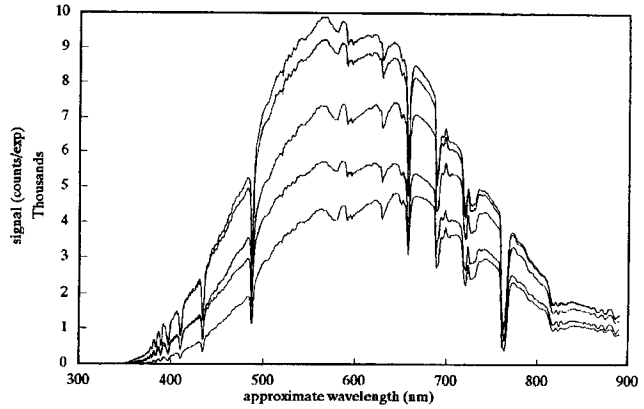

Fig. 4. Spectra of Sirius observed with the UVIZ at Cambridge on 7 February 1994. The different spectra are at different elevation angles, 21, 20, 16, 13, and 9°, with the smallest signal being at the lowest elevation. Integration time of each spectrum was 30 min.

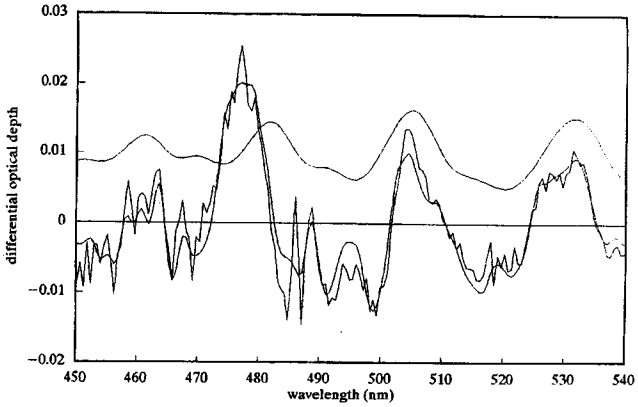

Fig. 5. Analysis of the ratio of the two spectra in Fig. 4 (Sirius at Cambridge on 7 February 1994). The lower traces are the measured (noisier) and fitted (smoother) differential optical depths (see text). The upper trace is the cross section of ozone, smoothed by the spectral resolution of the spectrometer and multiplied by the amount of ozone from the fit, displaced for clarity. Other absorbers are NO_2, H_2O, and O_4.

the buried part and just under the apparatus where the triangulation pieces had the minimum potential to cause drift. The vertical legs of the frame could be broken apart near their tops, so that new timbers of 1.2-m length could be inserted each year. Figure 2 shows the result at Halley.

5. Sample Measurements

Before deployment at Halley, we took measurements with the UVIZ from Cambridge, where it was mounted on a meteorological tower to gain good views close to the horizon. Figure 4 shows some spectra of Sirius from this test period. The ratio of signal-to-statistical noise in each pixel, equal to the square root of the number of electrons, can be calculated from the figure given the gain (1 digitizer count = 22 electrons) and the number of exposures, in this case 27. Hence at its maximum at 560 nm, the signal-to-noise ratio of the largest spectrum in Fig. 4 exceeds 2400, near the center of the ozone band at 503 nm it is 2100, and that of the smallest spectrum is 1300.

The spectral analysis scheme[5,6] performs a wavelength calibration before it interpolates one spectrum onto the pixel grid of the other so that their ratio can be found. The logarithm of this ratio is the optical depth that contains broad spectral features created by molecular (Rayleigh) and aerosol extinction as well as fine structure as a result of absorbing gases. The broad features are removed by a high-pass filter in wavelength space to produce the so-called differential optical depth.[7] This should equal the sum of {[cross section times (amount in signal spectrum minus amount in reference spectrum)] for all absorbers at each wavelength, plus instrument noise, plus systematic errors}. This, of course, depends on whether the cross sections have been similarly high-pass filtered and smoothed by the spectral resolution of the spectrometer. Cross section is defined as the absorptivity per molecule per unit area as measured in the laboratory.

Hence a multiple least-squares fit is performed to determine the slant column amounts. Figure 5 shows the result of this process in the ozone spectral region for the ratio of the smallest-to-largest spectra in Fig. 4. From the signal-to-noise ratios of the spectra, at 503 nm the statistical noise in the observed optical depth is 9×10^{-4}, which is equivalent to a peak-to-peak variation of ~0.004. This is consistent with the differences between the observed and fitted optical depths (the residuals) at 503 and 521 nm, showing that systematic errors in the spectra are not significant there. However, larger residuals, such as those at the Balmer line at 486 nm (although this line is excluded from the fit), illustrate that there are still systematic errors in some parts of the spectrum. These are probably due to stray light, which would give smoothly varying offsets to the zero of the spectra. Future research will attempt to model such offsets and retrieve their size from the spectra.

Figure 6 shows the amounts deduced from all the spectra on the night illustrated in Fig. 4. In our earlier study observing Vega,[5] we averaged several adjacent spectra to produce a pair of spectra at high and low elevations. However, this procedure does not minimize statistical error and has the additional disadvantage that error statistics cannot be tested. Instead, we now use Langley plots such as those in Fig. 6, and the least-squares slope and its error give the amount of ozone and its error directly; the differences from the line are a test of the validity of the error bars on the individual points. Here, the error in the slope from a weighted regression, which uses the differences from the line rather than the error bars, was within 1 DU (Dobson Unit) of the error from the standard weighted least-squares fit, hence the error bars are representative of the true errors (1 DU = 2.6818×10^{16} molecules cm^{-2}, a unit in common use in atmospheric science). The slope of the line is a vertical ozone amount of 374 ± 25 DU compared with 392 DU measured by a nearby zenith-sky spectrometer on the same evening.

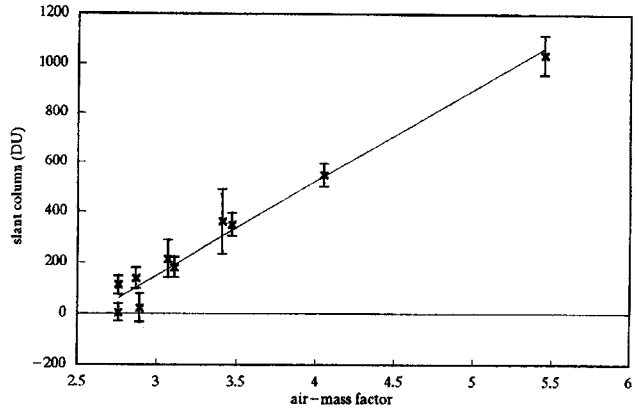

Fig. 6. Slant columns of ozone analyzed from all spectra for the night of 7 February 1994 (Sirius at Cambridge) plotted against the ratio of the slant path length to the vertical path length (AMF) calculated for the elevation of Sirius and for an absorber at 25 km. Error bars are those due to the residuals in the spectral fit, assuming they are random. The line is the weighted least-squares fit to the points and has a zero slant column when the AMF is 2.60. In such a Langley plot, the column should be zero at the AMF of the reference spectrum, here equal to 2.72. One Dobson Unit (DU) is 2.6818×10^{16} molecules cm^{-2}.

During shipment to Antarctica, the detector enclosure leaked, so that it is now at approximately −10 °C rather than −55 °C. Hence it has dark current, previously insignificant, whose noise significantly increases the total noise when signals are small. Figure 7 shows the increased noise in the spectra of Sirius from Halley compared with Fig. 4. The increased noise is also obvious in the spectral analysis of Fig. 8 and in the size of the error bars in Fig. 9. However, Fig. 9 shows how the clearer skies of Antarctica allow the UVIZ to observe Sirius much closer to the horizon than in Cambridge—the range of air-mass factor (AMF) is double that of Fig. 6 (AMF is the ratio of lengths in the slant path to the vertical path).

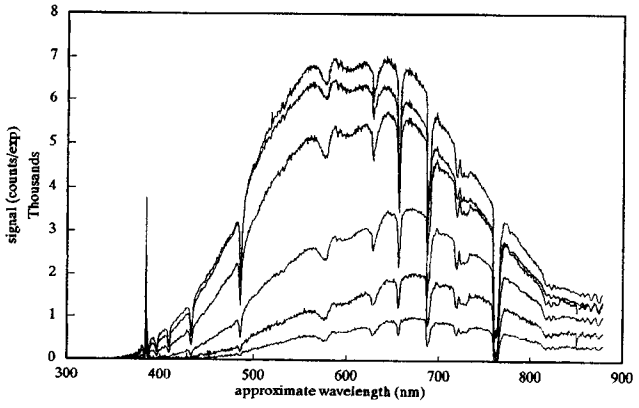

Fig. 7. Same as Fig. 4 but at Halley in Antarctica on the night of 2 August 1995 and at elevation angles between 2.4° and 14°. The spectra are noisier than those of Fig. 4 because air leaked into the evacuated detector encapsulation during shipping, so that the detector could not be cooled completely. Its warmer temperature (approximately −10 °C) means that the detector has more dark current.

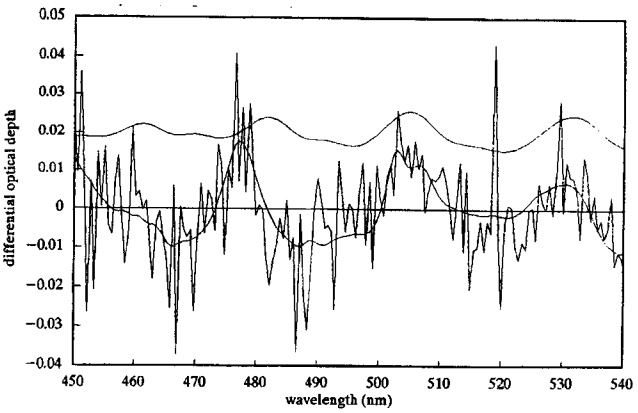

Fig. 8. Same as Fig. 5 except for Sirius at Halley on 2 August 1995. Despite the noisy spectra, the error in slant amount of ozone that is due to residuals in the fit is <35% and much of this is an artifact of a too large emission spike at 519 nm caused by a spectral lamp on a building.

In Fig. 9 the errors on the points are larger than the differences from the line, because there is emission from a spectral lamp on a nearby building, which is evident as small upward spikes on the larger spectra in Fig. 7 at 519 nm (spectral lamps are used on buildings to conserve power). Figure 8 shows that the emission at 519 nm anticorrelates with part of the ozone cross section, reducing the ozone slant columns and increasing the residuals in the spectral fit and so increasing the error bars. In Fig. 9, the two points with the smallest AMF have fortuitously similar emissions to the reference spectrum, hence their smaller error bars and realistic amounts of ozone. Points with an AMF of between 3 and 9 have differences from the line that are much less than the error

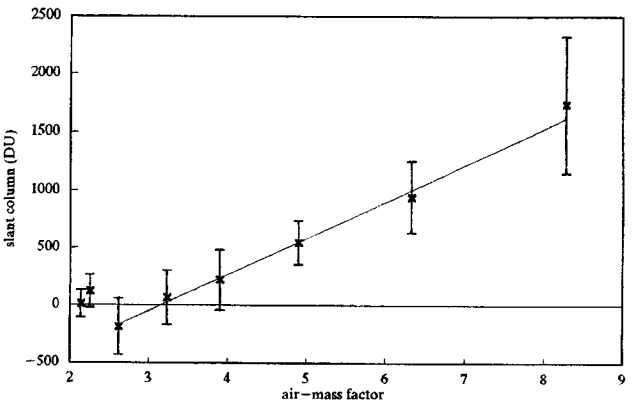

Fig. 9. Same as Fig. 6 except for Sirius at Halley on 2 August 1995. The line is the weighted least-squares fit to points with an AMF greater than 2.5; see text for discussion. Points at AMF's of 10.1 and 11 are not shown because they add little information: their error bars exceed ±2000 DU because of weaker signals within 3° of the horizon. Nevertheless, the range of the AMF is double that of Fig. 6.

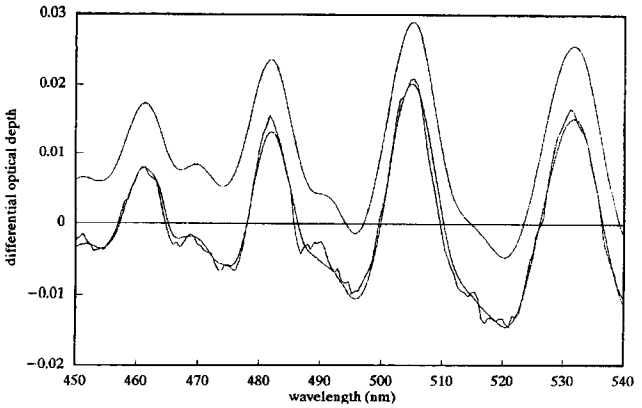

Fig. 10. Same as Fig. 5 except for the zenith sky at Halley during the morning twilight on 6 September 1995 at a solar zenith angle of 91.2°. Note the high quality of the data; the dark current is still small compared to the signals from the sunlit zenith sky.

bars and all the slant columns are too small, as evidenced by the AMF when the slant column is zero.

However, this illustrates the power of the Langley plot: the true error on the points can be discerned from the differences from straight-line fits, and points that contain artifacts are apparent. The slope of the line through the points with an AMF between 2.5 and 9 is 315 DU, with an error from a weighted regression of 11 DU. (We used the differences from the line rather than the error bars to determine the magnitude of the error in the slope). Addition of the points at AMF's of 10.1 and 11 (not shown) gives a similar value of 313 DU, but the error is increased to 27 DU because of their large differences from the line, which is consistent with large error bars. The closest lunar Dobson measurement was 221 ± 10 DU, taken 6 nights later.

Analyses of Sirius's spectra with the UVIZ can probably be improved by

(i) Measuring the dark current for a long period of time, then scaling it either by shorter measurements of dark current made several times each night or by the apparent signal at 260 nm in the sky spectrum of the detector, instead of the current medium-length measurements taken once each night.

(ii) Not subtracting the sky signal at all and fitting some sample measurements of aurora as cross sections. It is possible that errors in such a fit would be less than the errors introduced by the dark current in the sky spectrum.

(iii) Fitting the lamp spectrum as a cross section.

Such possible improvements, the accompanying comparisons with other measurements of ozone, and the search for possible seasonal variations in the comparison are beyond the scope of this paper. However, analyses of zenith-sky spectra from Halley need no such improvement. Figure 10 illustrates their excellent quality. They are significantly less noisy than comparable spectra with ambient detectors, despite the increased dark current.

We thank Pete Edgley for the scheme of the control computers and for the initial control software, much of which was still in use after 4 years of further development; Bryan Causton for his innovation with some details of mechanical design; and Kathy Preston for assistance with software for the Langley plots. DJF was supported by a studentship from the Natural Environment Research Council (NERC) and EKS by a grant from the NERC.

References

1. H. K. Roscoe, R. A. Freshwater, R. Wolfenden, R. L. Jones, D. J. Fish, J. E. Harries, and D. J. Oldham, "Using stars for remote sensing of the Earth's stratosphere," Appl. Opt. **33,** 7126–7131 (1994).
2. J-P. Pommereau and F. Goutail, "Stratospheric O_3 and NO_2 observations at the southern polar circle in summer and fall 1988," Geophys. Res. Lett. **15,** 895–897 (1988).
3. H. K. Roscoe, J. A. C. Squires, D. J. Oldham, A. Sarkissian, J-P. Pommereau, and F. Goutail, "Improvements to the accuracy of zenith-sky measurements of total ozone by visible spectrometers," J. Quant. Spectrosc. Radiat. Transfer **52,** 639–648 (1994).
4. H. K. Roscoe, "A star-pointing UV–visible spectrometer for polar stratospheric measurements," in *Proceedings of the First European Workshop on Polar Stratospheric Ozone Research*, J. A. Pyle and N. R. P. Harris, eds. (Commission of the European Communities, Brussels, 1991), pp. 91–94.
5. D. J. Fish, R. L. Jones, R. A. Freshwater, H. K. Roscoe, D. J. Oldham, and J. E. Harries, "Total ozone measured during EASOE by a UV–visible spectrometer which observes stars," Geophys. Res. Lett. **21,** 1387–1390 (1994).
6. D. J. Fish, "Measurements of stratospheric composition using ultraviolet and visible spectroscopy," Ph.D. dissertation (University of Cambridge, Cambridge, UK, 1994).
7. M. Q. Syed and A. W. Harrison, "Ground based observations of stratospheric nitrogen dioxide," Can. J. Phys. **58,** 788–802 (1980).